Flow Cytometry Analysis of Free Intracellular NAD$^+$ Using a Targeted Biosensor

Jared M. Eller,[1] Melissa L. Stewart,[2] Alexandria J. Slepian,[2] Sheila Markwardt,[3] Jack Wiedrick,[3] Michael S. Cohen,[4] Richard H. Goodman,[2] and Xiaolu A. Cambronne[1,5]

[1]Department of Molecular Biosciences, University of Texas at Austin, Austin, Texas
[2]Vollum Institute, Oregon Health & Science University, Portland, Oregon
[3]Biostatistics and Design Program, Oregon Health & Science University, Portland, Oregon
[4]Department of Physiology and Pharmacology, Oregon Health & Science University, Portland, Oregon
[5]Corresponding author: *lulu@austin.utexas.edu*

Flow cytometry approaches combined with a genetically encoded targeted fluorescent biosensor are used to determine the subcellular compartmental availability of the oxidized form of nicotinamide adenine dinucleotide (NAD$^+$). The availability of free NAD$^+$ can affect the activities of NAD$^+$-consuming enzymes such as sirtuin, PARP/ARTD, and cyclic ADPR-hydrolase family members. Many methods for measuring the NAD$^+$ available to these enzymes are limited because they cannot determine free NAD$^+$ as it exists in various subcellular compartments distinctly from bound NAD$^+$ or NADH. Here, an approach to express the sensor in mammalian cells, monitor NAD$^+$-dependent fluorescence intensity changes using flow cytometry approaches, and analyze data obtained is described. The benefit of flow cytometry approaches with the NAD$^+$ sensor is the ability to monitor compartmentalized free NAD$^+$ fluctuations simultaneously within many cells, which greatly facilitates analyses and calibration.

Keywords: ARTD • CD-38 • circularly permutated fluorescent protein • fluorescent sensor • genetically encoded biosensor • metabolite • NAD$^+$ • nicotinamide adenine dinucleotide • PARP • sirtuin

How to cite this article:
Eller, J. M., Stewart, M. L., Slepian, A. J., Markwardt, S., Wiedrick, J., Cohen, M. S., Goodman, R. H., & Cambronne, X. A. (2018). Flow cytometry analysis of free intracellular NAD$^+$ using a targeted biosensor. *Current Protocols in Cytometry*, e54. doi: 10.1002/cpcy.54

INTRODUCTION

In eukaryotes, the intermediary metabolite, nicotinamide adenine dinucleotide, predominantly exists as its oxidized form (NAD$^+$), serving two major cellular roles that are evolutionarily conserved (Verdin, 2015; Yang & Sauve, 2016). One role for NAD$^+$ is in oxidoreductive (redox) reactions, and a key example includes NAD$^+$ fueling the Krebs/citric acid cycle to ultimately drive ATP production. The NAD$^+$/NADH ratio controls flux through these pathways, and as several of the steps are reversible, the concentration of NAD$^+$ may contribute to the directionality of these reactions as well. The majority of intracellular NAD$^+$ is engaged in redox reactions and is thus tightly

CURRENT PROTOCOLS A Wiley Brand
Current Protocols in Cytometry e54
Published in Wiley Online Library (wileyonlinelibrary.com).
doi: 10.1002/cpcy.54

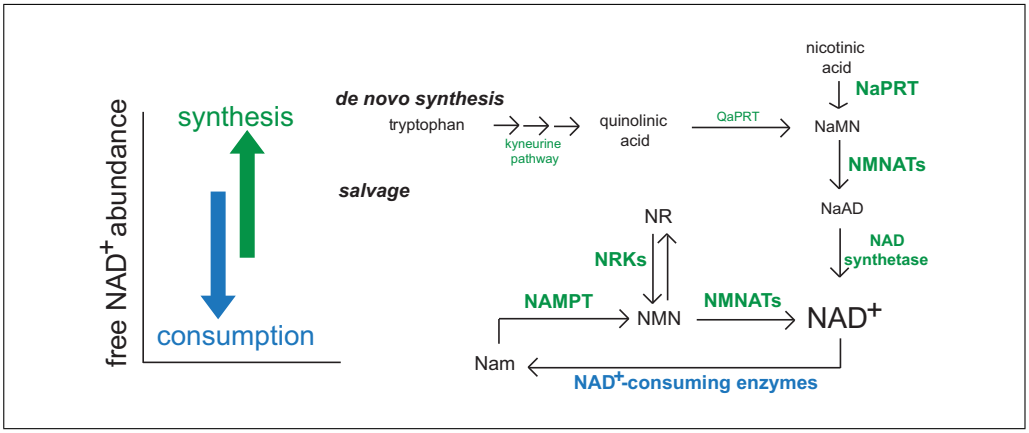

Figure 1 Regulation of NAD^+ steady-state concentrations. Free intracellular NAD^+ pools are regulated predominantly by biosynthetic (green) and consumption (blue) pathways, which synthesize or turn over NAD^+ molecules, respectively. In mammalian cells, NAD^+ synthesis largely depends on the salvage pathway. Thus, the specific targeting of the mammalian salvage pathway through inhibition of NAMPT results in robust depletion of NAD^+ abundance in the subcellular compartments tested here because resident consuming mechanisms are left intact. QaPRT, quinolinate phosphoribosyltransferase; NaMN, nicotinic acid mononucleotide; NMNAT, nicotinamide mononucleotide adenylyltransferase; NaAD, nicotinic acid adenine dinucleotide; NR, nicotinamide riboside; NMN, nicotinamide mononucleotide; NRK, nicotinamide riboside kinase; Nam, nicotinamide.

associated with protein (Holzer, Lynen, & Schultz, 1956; Bucher & Klingenberg, 1958; Williamson, Lund, & Krebs, 1967). Equally important for cellular fitness is the distinct role of NAD^+ as a required substrate for a broad class of enzymes, termed NAD^+-consuming enzymes. In mammals, these include 7 sirtuin deacylase family members, 17 ADP-ribose transferases (PARP/ARTD family members), and at least 3 cyclic ADP-ribose hydrolases (Gerdts, Brace, Sasaki, DiAntonio, & Milbrandt, 2015; Houtkooper, Cantó, Wanders, & Auwerx, 2010). These enzymes cleave the glycosidic linkage between the nicotinamide and ribose moieties, resulting in the consumption of an NAD^+ molecule for each enzymatic cycle. As such, NAD^+-consuming enzymes depend on the local availability of free NAD^+ molecules.

Many human pathologies—including neurodegeneration, cardiovascular disease, metabolic syndrome, and cancer—are linked to misregulated NAD^+-consuming enzymes (Houtkooper et al., 2010; Verdin, 2015; Yang & Sauve, 2016). The local concentration of NAD^+ therefore has been proposed to contribute to these diseases by being limiting for specific NAD^+-consuming enzymes, many of which have $K_M(NAD^+)$ values that approximate local physiological concentrations of NAD^+ (Houtkooper et al., 2010). The challenge is being able to measure the amount of free NAD^+ in cells that is available to NAD^+-consuming enzymes in biologically relevant contexts. The abundance of the protein-bound NAD^+ creates a challenge when assessing the amount of free NAD^+ available as substrate. The protein-bound NAD^+ in redox reactions does not turn over, thus steady-state levels of the bound fraction minimally fluctuate under normal physiology. As such, the abundance of the protein-bound fraction may overwhelm any detection of free NAD^+ fluctuations in total measurements. The free NAD^+ fraction, in contrast, is susceptible to steady-state changes through the balance between its biosynthetic and consumption pathways (Fig. 1).

Local concentrations of NAD^+ can differ in different biological compartments, and subcellular concentrations of NAD^+ can be regulated independently through biosynthetic pathways or depleted by local consuming enzymes. Understanding this would provide (1) an important framework for understanding NAD^+ regulation; (2) information about where, when, how, and the extent to which local free NAD^+ concentrations may be

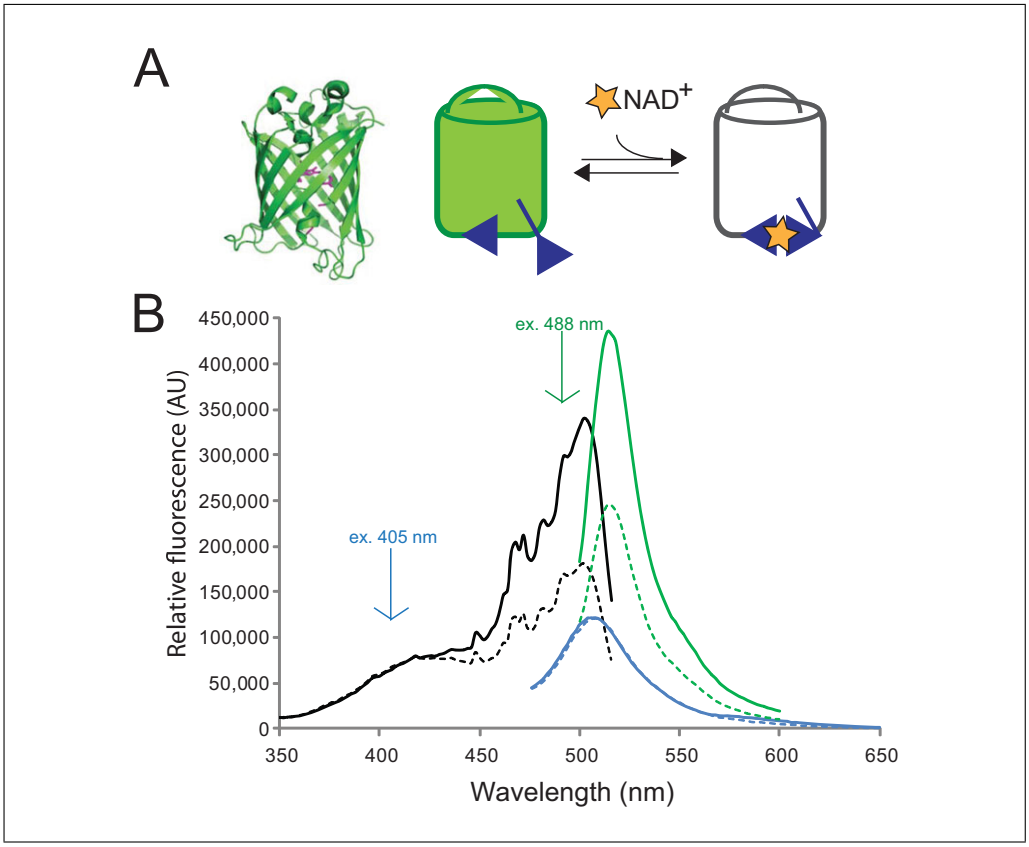

Figure 2 Characteristics of the NAD^+ sensor. (**A**) (Left) Structural depiction of a circularly-permuted fluorescent protein similar to cpVenus (modified PDB: 3EVP). Highlighted in magenta are the new N- and C- termini (formally residues 145 and 146, respectively), which have been relocated closer to residues that constitute the chromophore centered in the beta-barrel. (Right) When the bi-partite NAD^+-binding pocket of the sensor (blue) binds NAD^+ (yellow star) the fluorescence of the sensor decreases. (**B**) The NAD^+ sensor harbors a primary peak in its excitation spectrum monitored at 530 nm (black), which can be excited at 488 nm to produce fluorescence ~520 nm (green). A secondary excitation peak is excitable at 405 nm to yield fluorescence ~510 nm (blue). The presence of NAD^+—shown here by addition of 500 μM NAD^+ (dotted line)—decreases the fluorescence following 488 nm excitation but has minimal effect on the fluorescence from excitation at 405 nm.

limiting in disease, and (3) help identify treatments or approaches that may be able to influence local free NAD^+ availability. Towards this goal, a genetically encoded fluorescent sensor for free NAD^+ that can be localized to specific subcellular compartments for direct measurements has been developed (Fig. 2) (Cambronne et al., 2016). Versions of the NAD^+ biosensor targeted to the nucleus, cytoplasm, or mitochondrial matrix have been generated to monitor the steady-state levels of free NAD^+ in these specific subcellular compartments. Details about the design of the sensor can be found in Cambronne et al. (2016).

The first protocol describes a transient approach for expressing the sensor from a plasmid (see Basic Protocol, steps 1 through 17) and for obtaining relative measurements of NAD^+ fluctuations (see Basic Protocol, steps 18 through 39). Additionally, statistical analyses to evaluate the significance of measured changes from experimental replicates are described (see Basic Protocol, steps 40 to 50). This transient transfection protocol works best with flow cytometry measurements where it is relatively easy to obtain a large population of fluorescent cells for evaluation. The Alternate Protocol covers how to create an in-cell calibration curve for interpolating cytoplasmic measurements obtained from flow cytometry (see Alternate Protocol, steps 16 through 27). It encompasses the experimental preparation, and how to monitor the sensor during the calibration. This method may be

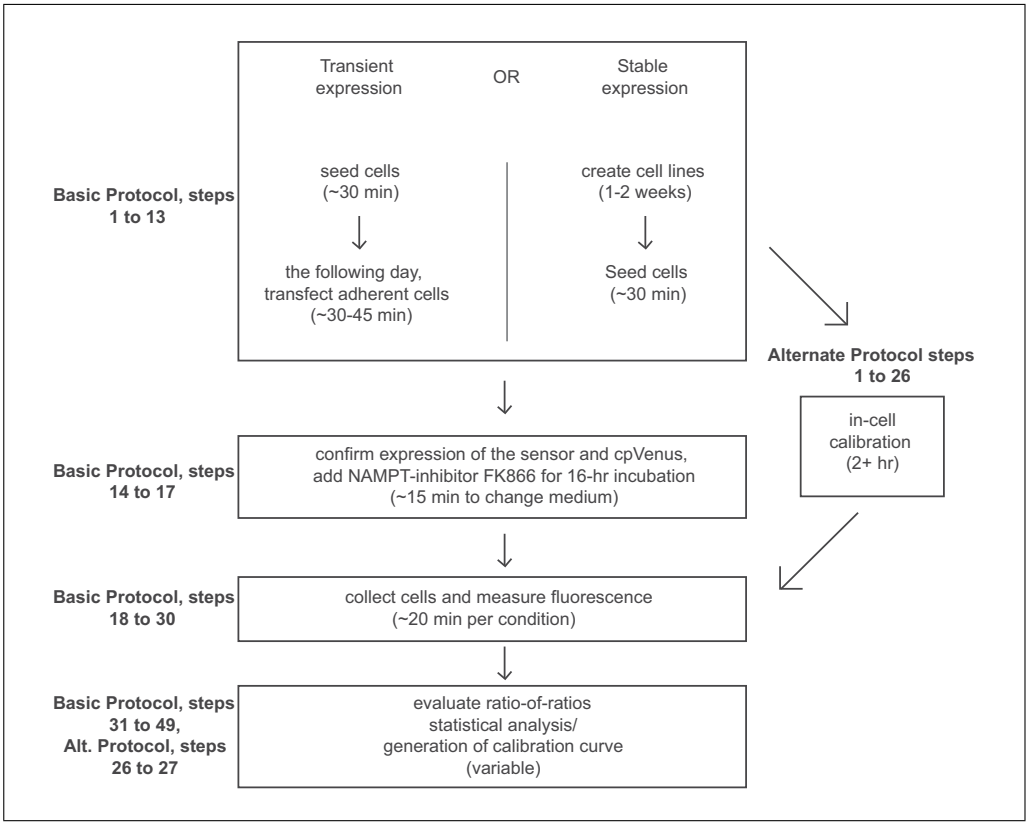

Figure 3 Flow chart outlining protocol steps.

more difficult for laboratories not experienced with cell culture or laboratories that do not wish to spend time creating the stably expressing line, but it does offer the ability to measure quantitative values of NAD^+ concentration. Figure 3 shows a diagram of the work-flow for each method.

BASIC PROTOCOL

TRANSIENT EXPRESSION OF THE NAD^+ SENSOR AND ANALYSIS VIA FLOW CYTOMETRY

Measurements of subcellular free NAD^+ are critical for understanding changes in the function and regulation of NAD^+-consuming enzymes within eukaryotic systems. By targeting a genetically encoded fluorescent biosensor to subcellular compartments, local free NAD^+ concentrations can be analyzed through flow cytometric methods. A description of how to express the NAD^+ sensor in mammalian HeLa cells and how to treat these cells with FK866 {N-[4-(1-benzoyl-4-piperidinyl)butyl]-3-(3-pyrindyl)-2Epropenamide} is also provided. FK866 is a highly specific small molecule inhibitor for nicotinamide phosphoribosyltransferase (NAMPT). By inhibiting the enzyme responsible for a rate-limiting step in mammalian NAD^+ biosynthesis (Revollo, Grimm, & Imai, 2004), NAD^+ concentrations can be effectively lowered through its depletion across cellular compartments and this reduction can be measured as an increase in fluorescence intensity with the sensor and flow cytometry (Cambronne et al., 2016).

Materials

HeLa cells (healthy, proliferating, and maintained in 10-cm dish or similar)
Dulbecco's phosphate buffered saline (DPBS) without calcium chloride and magnesium chloride (Thermo Fisher, cat. no. 14190-144)
0.05% (v/v) EDTA-Trypsin (Thermo Fisher, cat. no. 25300-062), store at –20°C
Cell culture growth medium (see recipe)

Lipofectamine 2000 (Thermo Fisher, cat. no. 11668-019), store at 4°C
Serum-free Opti-MEM medium containing HEPES, 2.4 g/liter sodium bicarbonate, and L-glutamine (Thermo Fisher, cat. no. 31985-070), store at 4°C
NAD^+ sensor purified plasmid DNA (2 µg for 35-mm dish; 20 µg for 10-cm dish)
cpVenus purified plasmid DNA (2 µg for 35-mm dish; 20 µg for 10-cm dish)
Mitotracker Red CMXRos (Thermo Fisher, cat. no. M7512)
Hoechst 33342 (Thermo Fisher, cat. no. H3570)
50 mM FK866 in DMSO (see recipe)
Dimethyl sulfoxide (DMSO, Fisher Chemicals, cat. no. 67-68-5)

37°C, 5% CO_2 tissue culture incubator (Eppendorf New Brunswick Galaxy 170S CO_2 cell culture incubator or similar)
Inverted wide-field light and fluorescent microscope with Dapi, GFP, and DsRed compatible filter sets (Sole SM II light engine or similar)
Hemacytometer (Fisher Scientific, cat. no. 0267110) or digital cell counter
6-well tissue culture–treated plastic plates (Corning, cat. no. 353406)
Serological pipets:
- 2-ml aspirating pipet (Fisher, cat. no. 13-678-11C)
- 5-ml pipet (Fisher, cat. no. 13-678-11D)
- 10-ml pipet (Fisher, cat. no. 13-678-11E)
- 25-ml pipet (Fisher, cat. no. 13-678-11)

Portable pipet-aid (Corning, cat. no. 4099 or similar)
Eppendorf Research Plus Micropipette in sizes P10, P20, P200, and P1000 or similar
Barrier tips:
- 10-µl (USA Scientific, cat. no. 1121-2710)
- 20-µl (USA Scientific, cat. no. 1123-1710)
- 200-µl (USA Scientific, cat. no. 1120-8710)
- 1000-µl (USA Scientific, cat. no. 1122-1730)

Flow cytometer (BD LSR II, BD Fortessa, or similar)
- Filer set: 405-2; Laser: 405 nm; Detector 525 ± 25 nm
- Filter set: 488-1; Laser: 488 nm; Detector 530 ± 15 nm
- Filter set: 561-3; Laser: 561 nm; Detector: 670 ± 15 nm

40- to 70-µm nylon mesh
FlowJo data analysis software version 10 (Microsoft or similar)
STATA-14 statistical analysis software (or similar)

NOTE: Cell lines should be regularly checked to ensure authenticity and lack of mycoplasma infection via PCR. All steps involved with seeding cells should be performed in a biosafety cabinet with sterile technique to prevent contamination of cells.

Seed cells

1. Calculate the number of experimental conditions needed.

   Before starting, ensure HeLa cells are healthy, free of mycoplasma contamination, and have been proliferating steadily.

2. Aspirate the medium from HeLa cells in 10-cm plate.

   Do not leave cells to dry out without medium or PBS.

3. Wash cells with 10 ml DPBS and then remove DPBS. Add 1 ml of 0.05% (v/v) EDTA-trypsin to cells and incubate in a 37°C, 5% CO_2 incubator until all cells are detached. Verify that cells have completely detached using an inverted wide-field light microscope.

   To keep cells healthy, do not trypsinize cells >5 min.

Cells should be rounded up or free-floating before continuing.

4. Quench trypsin by adding 10 ml of complete cell culture growth medium to dish. Triturate cells into a single-cell suspension.
5. Use a hemacytometer or digital cell counter to count and calculate number of cells per milliliter (dilution of cells may be necessary to accurately count).
6. Determine number of cells needed for the total experiment. Start with ~250,000 HeLa cells per well of a 6-well plate (each well holds 2 ml of volume). Dilute cell stock appropriately in complete cell culture growth medium and seed HeLa cells in a 6-well plate at a concentration such that they will reach ~50% confluency in 24 hr.

Transfect cells

7. Twenty-four hours after seeding, transfect HeLa cells with expression plasmids for the sensor or cpVenus controls. Confirm that cells are ~50% confluent using a light microscope.
8. In a sterile tissue culture hood, prepare a master mix containing Lipofectamine 2000 transfection reagent diluted in serum-free Opti-MEM medium. For each well, prepare a ratio of 5 µl Lipofectamine 2000 in 200 µl Opti-MEM medium for 2 µg of total DNA transfected; e.g., for four transfections, prepare 20 µl Lipofectamine 2000 in 800 µl of Opti-MEM medium. Vortex to mix.

   Lipofectamine 2000 reagent should be kept cold on ice until use.

   Serum-free Opti-MEM medium should be a peach color to indicate correct pH.

9. Prepare separate tubes of DNA diluted in Opti-MEM medium: one containing the expression plasmid DNA for the sensor and the other containing the expression plasmid DNA for cpVenus diluted in Opti-MEM medium. For each well of a 6-well plate, dilute 2 µg DNA in 200 µl Opti-MEM medium; e.g., for two transfections with the sensor plasmid representing treated and untreated conditions, dilute 4 µg sensor plasmid in 400 µl Opti-MEM medium. Vortex to mix well.
10. Add 400 µl Lipofectamine 2000 transfection master mix to the tubes containing either the diluted sensor or cpVenus plasmids. Vortex to mix well and incubate 20 min at room temperature.
11. After incubation, add 400 µl per well of the Lipofectamine/DNA transfection mixture dropwise onto the already seeded HeLa cells.
12. Incubate cells 2 hr in the 37°C, 5% CO_2 incubator.
13. After 2 hr, remove medium containing transfection mixture and replace with new complete cell culture growth medium.

    Increased incubation with the transfection mixture may be toxic for this cell type.

14. Confirmation of a successful transfection can be observed with fluorescence microscopy in the green channel by the next day. Transfected cells should fluoresce green and localize to expected subcellular compartments.

    Do not leave cells out of the incubator for >10 min as this may negatively affect their health.

    It is important to confirm that the sensors are localized to expected subcellular compartments via microscopy. Broad illumination with a GFP-compatible filter is sufficient to visualize the sensor. Either prior to the experiment or in parallel, the subcellular localization of the sensor in live cells can be correlated with nuclear Hoechst 33342

Table 1 Minimal Experimental Conditions Required for a Single Assay[a]

	To be transfected		
Treatment	cpVenus control	NAD^+ sensor	No transfection
0 nM FK866	Condition 1	Condition 2	Condition 5[b]
10 nM FK866	Condition 3	Condition 4	Optional

[a]This table outlines the minimum experimental conditions required to evaluate NAD^+ changes in a single subcellular compartment. To evaluate multiple sensors that target distinct subcellular localizations, an equivalently targeted cpVenus control is required and a similar set of conditions are needed for each sensor.
[b]This control will be used to set up cytometry gates and distinguish the cells expressing the sensor compared to untransfected cells during fluorescence measurements.

staining and mitochondrial staining with red mitotracker; both dyes are cell permeable and amenable to use in live cells. Subcellular localization of the sensor in live cells can also be estimated by comparison of the expression pattern of the sensor relative to bright-field images.

Treat cells with small molecule NAMPT inhibitor FK866

15. Twenty-four hours post-transfection, treat cells with freshly diluted 10 nM FK866. Freshly dilute FK866 from the DMSO stock in medium with serial dilutions from 50 mM down to 10 nM. The 0 nM FK866 treatment should include serially diluted DMSO similar to the 10 nM FK866 treatment to serve as a control.

16. Aspirate medium from transfected HeLa cells and gently replace with either 0 or 10 nM FK866 in complete cell culture growth medium as indicated in Table 1.

17. Incubate cells 16 hr in a 37°C, 5% CO_2 incubator.

Depending on the biological compartment and cell type, differences in the rate of NAD^+ depletion have been observed (Cambronne et al., 2016). As a reasonable starting point for these experiments, a 16-hr incubation is recommended, where depletion in most compartments has been consistently observed. When HeLa cells are incubated with FK866 for >18 hr, cell morphological changes in the population have been observed, which indicate compromised cellular health (Fig. 4). To ensure that relatively healthy cells are evaluated and to prevent misinterpretation by secondary effects, FK866 treatments are limited to ≤16 hr.

Prepare cells for flow cytometry evaluation

18. Prepare and label flow cytometry sample tubes on ice.

19. Remove cell culture growth medium from cells and gently wash one time with PBS.

This preparation must be within 5 to 10 min from start to finish due to the analysis being performed on live cells out of the incubator. If more samples are to be processed than can be handled in this time, trypsinize, collect cells, and analyze in small batches (i.e., one 6-well plate at a time). From here onward, contamination of the cell culture is no longer a consideration and cells can be prepared for analysis outside of the biosafety cabinet if needed.

20. Add 100 µl of 0.05% EDTA-trypsin to each well and incubate in a 37°C, 5% CO_2 incubator until cells come off the plate easily.

21. Add 400 µl freshly prepared complete cell culture growth medium to each well to quench the trypsin.

It is critical to ensure that the medium used to resuspend cells (complete cell culture growth medium including HEPES) is within near-neutral pH. If it contains phenol red, the medium should be orange-red in color without any traces of pink or magenta.

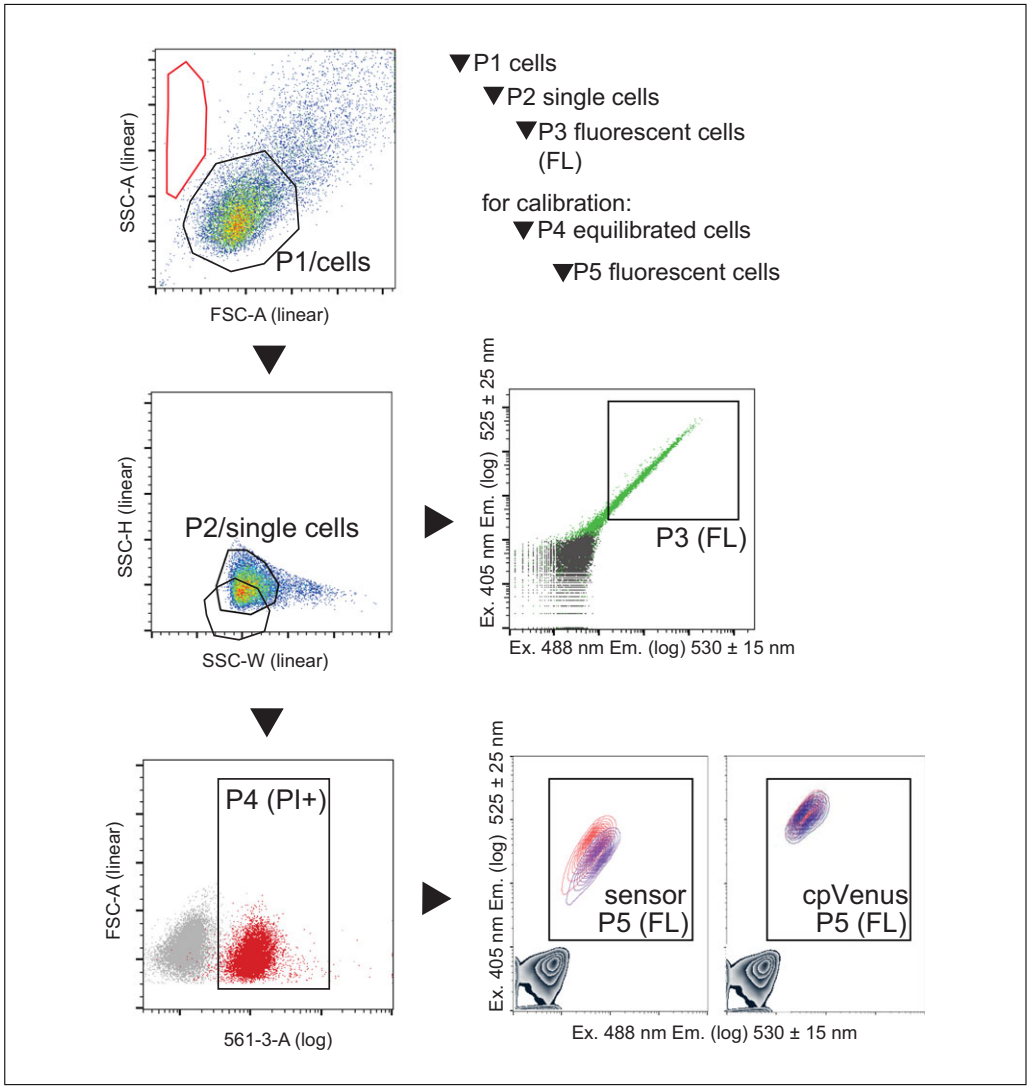

Figure 4 Hierarchical gates to evaluate fluorescent cells. Gates are applied identically to all samples. The P1 gate outlines the uniform population of HeLa cells for evaluation (typically >75% of total events). Under these specific conditions, events in the red region represent cellular debris or mechanically disrupted cells; if >50% of events are in this region it indicates an overall unhealthy sample. From the P1/cell population, single cells are identified by the P2 gate using their size distribution (typically >90% of P1). The P3/fluorescent population is derived from the P2/single cell population. The P3 fluorescent cell population is defined by a gate that excludes non-fluorescent cells in the untransfected sample (gray) and includes transfected cells (green, typically >50% of P2). There should be ~10,000 events in P3 for an accurate evaluation. To calibrate the sensor in cells, an additional gate is required to identify the permeabilized and equilibrated cells. This P4 gate (typically >85% of P3) is derived from uniform, single cells in P2, and is delineated by equilibrated intracellular propidium iodide (PI). Fluorescence is then evaluated in P5, which is derived from P4. In this example, a gray density contour plot in the lower left quadrant represents cells that do no express either sensor or cpVenus. Cells that express either sensor or cpVenus populate P5, and the fluorescence of the populations treated with either equilibrated buffer (red) or 500 μM NAD^+ (indigo) are overlaid. Data was collected on a BD Fortessa flow cytometer and analyzed on FlowJo V10 software.

HEPES is necessary in the medium to buffer the cell suspension during flow analysis, which is typically performed on the bench outside of an incubator.

22. Triturate with a 1-ml pipet tip to obtain single-cell suspension and immediately transfer to sample tube on ice.

Including serum in the medium and keeping cells on ice help to prevent cells from clumping.

Table 2 Measurements Needed for Flow Cytometry Analysis

Name	Scale	Approximate voltage guidelines for HeLa cells[a]
SSC-A	Linear	~275
FSC-A	Linear	~220
SSC-H	Linear	No recommendation
SSC-W	Linear	No recommendation
Filter set: Ex. 488 nm, Em. 530 ± 15 nm	Log	~275
Filter set: Ex. 405 nm, Em. 525 ± 25 nm	Log	~250

[a]The voltage guidelines provided here are only indicated as aides for setting up a template. The user must adjust the voltage such that all measurements are on-scale for the instrument's specific lasers and setup. Different instruments may have different voltage settings or may not have voltage controls.

Perform flow cytometry measurements

23. Refer to Table 2 for instrumental guidelines and the data parameters to collect.
24. Ensure that the lasers have been warmed up and are stabilized, and that lines have been cleaned from previous users with bleach, detergent, and water. Ideally, the template is pre-loaded onto the instrument so that it can be immediately processed. If not, save a new template from the analysis when finished. When choosing the speed to perform the cytometry analysis, rapid evaluation of fluorescence across samples is preferable, so it is recommended to run samples on "high," if possible.
25. (Optional) Ensure that the cells are sufficiently separated as a single-cell suspension to prevent the flow from clogging. Filter cell suspension through a 40- to 70-µm nylon mesh to ensure that no significant clumps are present in the sample.
26. Collect the first data from untransfected HeLa cells (condition 5, Table 1) to ensure the gates have been accurately drawn around the three populations.

    For the HeLa sample, confirm that cells appear in P1 and P2 but not in P3 (Fig. 4, gray population; gates P1 through P3 are utilized for this protocol; gates P1 through P5 are utilized for the Alternate Protocol).

27. Evaluate the population of cells as a hierarchy to obtain fluorescent measurements from healthy, single, and transfected cells (Fig. 4). Adjust voltages of each laser per instrument and experiment based on untransfected HeLa cells (condition 5, Table 1). All cell gates should be centered within the plot. The P1 gate identifies the healthy cell population with relatively uniform forward and side scatter; *x*-axis is set to FSC-A (linear) and the *y*-axis to SSC-A (linear) (Fig. 4).
28. The P2 gate defines single cells and is derived from the P1 population in a new plot (Fig. 4). To perform a doublet-exclusion, select the P1 population for viewing and set the *x*-axis to SSC-W (linear) and the *y*-axis to SSC-H (linear). Draw the gate (P2) around the population on the left. This gate represents individual cells, as opposed to multiple cells stuck together that will appear as a group with a greater width.
29. The P3 gate is derived from the P2 population. P3 identifies cells that have been transfected and are fluorescent. The P3 gate is defined by exclusion of the untransfected, non-fluorescent cells in condition 5 (Fig. 4). Viewing the cells in P2 in a new plot, set the *x*-axis in log display for excitation at 405 nm and capture emission by filter set 525 ± 25 nm. Set the *y*-axis in log display to excite at 488 nm and capture emission with filter set 530 ± 15 nm. Draw a gate to the right and above the cell population in the HeLa sample, ensuring that any events in this gate are not included

(Fig. 4). This gate will represent the fluorescent, sensor or cpVenus-expressing cell populations, which will be unpopulated for untransfected HeLa cells.

30. The order of the remainder of samples is not critical but complete within 15- to 20-min sessions. It is necessary to collect at least 10,000 cells in P3 to rigorously evaluate the fluorescence of each sensor or cpVenus population. Save data from all events.

    This is a stage where one may pause the experiment. Once data has been collected, data can be analyzed at the convenience of the user.

Analyze fluorescence using FlowJo software

31. Export data in an FCS file format for analysis with a post-capture software such as FlowJo to determine the 488/405 nm fluorescence ratio per cell.

32. Open a new workspace and drag all FCS files (each representing a different experimental condition) into the workspace.

33. Double click the HeLa untransfected sample (condition 5, Table 1), which opens the data in a new window. Re-define the similar gates as those used to collect data in steps 26 to 28. Viewing the data as a density plot in pseudocolor is recommended (Fig. 4).

34. Once initial gates are defined, apply these gates to all samples to ensure that identical gating is performed on all samples. Confirm by checking for each condition that the gate is transferred and appropriately drawn such that it includes the correct cell population. If necessary, the gate can be redrawn and replaced in all samples with a larger gate.

    Confirm that a relatively equal number of cells (~10,000 cells) are being evaluated in the P3 gate across all experimental conditions, excluding the HeLa control sample.

35. Determine fluorescence ratio of 488 nm/405 nm per cell. In the FlowJo software, select Derive Parameters under the Tools tab. Enter the Formula by clicking Insert Reference to select the 488-nm measurement, click the ÷ key, and Insert Reference to select the 405-nm measurement.

    Obtaining the 488/405-nm measurement per cell is distinct from taking the average 488-nm fluorescence of the population and dividing by the average 405-nm fluorescence of the same population of cells. This number describes the level of fluorescence change due to NAD^+ (488 nm) compared to the measurement of the amount of sensor expressed (405 nm).

36. Apply this Derived value to All Samples. A histogram of the derived value should result in a defined peak. It is appropriate to use the geometric mean of this derived ratio as the fluorescence value for each experimental condition because fluorescence measurements are log-amplified. These ratiometric values can be exported into a table using the Table Editor function.

Analyze sensor data to determine the ratio of ratios

37. The Ratio of Ratios value represents the ratiometric measurement of the sensor with respect to its cpVenus control or relative to untreated controls. Divide the ratiometric 488/405-nm fluorescence value for the sensor by the corresponding value for the cpVenus control subjected to the same condition, e.g., the measurements for sensor and cpVenus both treated with FK866. This normalization accounts for any NAD^+ -independent fluorescence changes (Table 3).

Table 3 Example of How to Compare Ratiometric Measurements

Geometric mean 488/405 nm fluorescence values of each population						
	Nuclear cpVenus	Nuclear sensor	Cytoplasmic cpVenus	Cytoplasmic sensor	Mitochondrial cpVenus	Mitochondrial sensor
0 nM FK866	6.83	2.26	7.79	2.51	22.1	5.37
10 nM FK866	6.85	3.34	7.46	3.78	22.8	7.30
Option 1: Compared to cpVenus						
0 nM FK866	2.26/6.83 = 0.33		2.51/7.79 = 0.32		5.37/22.1 = 0.24	
10 nM FK866	3.34/6.85 = 0.49		3.78/7.46 = 0.51		7.3/22.8 = 0.32	
Fluorescence change	Nuclear		Cytoplasmic		Mitochondrial	
Ratio-of-ratios[a] (treated/untreated)	0.49/0.33 = 1.48		0.51/0.32 = 1.57[b]		0.32/0.24 = 1.32[b]	
Option 2: Compared to untreated						
	6.85/6.83 = 1.00	3.34/2.26 = 1.48	7.46/7.79 = 0.96	3.78/2.51 = 1.51	22.8/22.1 = 1.03	7.3/5.37 = 1.36
Fluorescence change	Nuclear		Cytoplasmic		Mitochondrial	
Ratio-of-ratios[a] (treated/untreated)	1.48/1.00 = 1.48		1.51/0.96 = 1.57		1.36/1.03 = 1.32[b]	

[a] The ratio-of-ratios provides a relative comparison to determine whether an NAD^+-dependent fluorescence change occurred. This table contains a normalization step first, then a ratio is being determined from the normalized values. The statistical significance of the change is evaluated with experimental replicates, described in Basic Protocol, steps 40 to 49. Because the comparison utilizes division, the order of the comparisons (either option 1, relative to cpVenus or option 2, relative to untreated control) does not matter.

[b] Values based on non-rounded numbers.

38. To discern whether relative NAD^+ changes have occurred, divide the ratio of ratios value determined in step 37 for treated cells by the analogous ratio of ratio value for untreated cells. With FK866 treatment, the fluorescence of the sensor is expected to increase in relative brightness. A relative increase in fluorescence indicates less free NAD^+, and is denoted by a relative value >1; therefore, more NAD^+ is indicated by a relative value <1 (see Tables 3 to 6).

39. To relate the measurement to an intracellular concentration, interpolate this ratio-of-ratios value to a standard curve (see Alternate Protocol).

Perform statistical analysis using STATA14 to evaluate significance of relative changes from experimental replicates

40. Organize data as shown in Tables 4 through 6. Use a comma-delimited file, e.g., filename.csv. Experimental replicates are grouped and indicated by numbers 1 to *n*. Input geometric mean fluorescence values under "fl." Treatment is designated with either "0" indicating untreated, or "1" indicating FK866-treated. cpVenus is designated with "0" and Sensor is designated with "1".

41. Import the data file under Text Data in the STATA14 software. Browsing to find the location where the file had been saved may be necessary. When uploaded correctly, the program will indicate it found four variables (columns) and *x* observations (number of rows). The uploaded data can also be verified by checking under Data Editor.

42. Perform a log transformation of the geometric mean fluorescence values to help control for variability. This can be accomplished by entering the following command: generate log_fl=log(fl).

    Use commands that reflect the exact case and format of the headings in the data file.

43. To denote that the data represents repeated measures (replicates), enter the following command: xtset experiment.

44. To apply the statistical model, enter the following command:

    xi:xtmixed log_fl i.sensor*i.treatment || experiment:, reml

45. A summary of the estimated results of the model will display in a format similar to what is shown in Tables 4 through 6. The values shown in these tables will be present as a readout from the program, including the coefficient (Coef.), the 95% confidence (95% Conf.), and the *p*-value described in later steps.

46. The estimate for the ratio of ratios across multiple experiments is represented by the third row, IsenXtre_1_1, also known as the statistical interaction (Tables 4 to 6). The *p*-value from this row represents the probability that—after controlling for any changes in the fluorescence of cpVenus—any observed difference in sensor fluorescence is indistinguishable from variation due to random sampling error. Thus, a small *p*-value represents situations where the "null" model is a poor explanation of the data. In these experiments, the *p*-values are <0.05.

47. To determine the mean fold change in fluorescence for the ratio of ratios across replicates, calculate the exponential of the coefficient (Coef.).

48. To examine the changes in the sensor and the changes in cpVenus independently, the estimates can be found as follows. For cpVenus, the estimate for the fluorescence change across replicates is represented by the row named _Itreatment_1

Table 4 Data and Statistical Analysis from Nuclear Sensor Replicates

Data represents biological replicates using transiently transfected nuclear sensor and nuclear cpVenus in HeLa cells[a]

Experiment	fl	Treatment	Sensor
1	9.97	0	0
1	10.00	1	0
1	3.78	0	1
1	6.45	1	1
2	6.83	0	0
2	6.85	1	0
2	2.26	0	1
2	3.34	1	1
3	6.70	0	0
3	7.28	1	0
3	2.30	0	1
3	3.56	1	1

Calculated statistical interaction table from STATA14 using REML[b]

log_fl	*Coef.*	*Std. Err.*	*z*	*P>* $\|z\|$	*[95% Conf.*	*Interval]*
_Isensor_1	−1.05	0.06	−17.09	0	−1.17	−0.93
_Itreatment_1	0.03	0.06	0.48	0.629	−0.09	0.15
_IsenXtre_1_1	0.42	0.09	4.89	**0**	0.25	0.59
_cons	2.04	0.16	12.73	0	1.73	2.36
_IsenXtre_1_1 + _Itreatment_1	0.45	0.061337	7.40	0	0.33	0.57

[a]Data are arranged for input into STATA14 statistical software. "0" represents cells treated with 0 nM FK866. "1" represents cells treated with 10 nM FK866. The fl values represent the geometric mean from 488/405 nm fluorescence ratio of the healthy, single HeLa cells measured by cytometry. Experiment, biological replicate; fl, 488/405 nm geometric mean fluorescent value; treatment, ±10 nM FK866; sensor, ±nuclear NAD^+ sensor.

[b]The *p*-value for the ratio-of-ratios across replicates (bold) is reported under the statistical interaction "_IsenXtre_1_1". This represents the fluorescence change following FK866 treatment in the nuclear sensor, relative to changes in cpVenus. Calculating the exponential of the coefficient value, Coef., represents the mean fold-change in fluorescence for the ratio-of-ratios across replicates, i.e., e^(0.42) = 1.52, 95% CI (e^0.25 – e^0.59) = 95% CI (1.28 to 1.80), $p < 0.001$.

The fluorescence change following FK866 treatment in nuclear cpVenus across replicates is represented by "_Itreatment_1": e^(coef) = e^(0.03) = 1.03, $p = 0.629$.

To calculate the average fluorescent change in the nuclear sensor independent of cpVenus, combine the "treatment" and "sensor X treatment interaction" using the lincom command (step 50). The combined values (blue) represents the change in the sensor: e^(coef) = e^(0.45) = 1.57, 95% CI (1.39 to 1.77), $p < 0.001$.

(Tables 4 through 6). In these experiments, the changes in cpVenus are not significantly different with FK866 treatment. The fold change can be calculated by taking the exponential of the coefficient in this row, and the 95% confidence interval can be similarly calculated by taking the exponential of the values in the column labeled "Coef."

49. To calculate the average fluorescent change in the sensor independent of cpVenus, combine the "treatment" and "sensor X treatment interaction" using the following command: lincom _IsenXtre_1_1 + _Itreatment_1. This generates a new table, which can be used to determine the reported *p*-value for this condition, calculate the fold-change by taking the exponential of the coefficient, and calculate the 95% confidence interval by taking the exponential of the values in the column labeled "Coef."

Table 5 Data and Statistical Analysis from Cytoplasmic Sensor Replicates

Data representing biological replicates using transiently transfected cytoplasmic sensor and cytoplasmic cpVenus in HeLa cells[a]

Experiment	fl	Treatment	Sensor
1	9.65	0	0
1	9.56	1	0
1	3.06	0	1
1	4.35	1	1
2	7.79	0	0
2	7.46	1	0
2	2.51	0	1
2	3.78	1	1
3	7.33	0	0
3	7.74	1	0
3	2.35	0	1
3	3.62	1	1

Calculated statistical interaction table from STATA14 using REML[b]

log_fl	*Coef.*	*Std. Err.*	*z*	*P*> |*z*|	*[95% Conf.*	*Interval]*
_Isensor_1	−1.14	0.03	−43.51	0	−1.19	−1.09
_Itreatment_1	0.00	0.03	0.02	0.982	−0.05	0.05
_IsenXtre_1_1	0.40	0.04	10.72	**0**	0.32	0.47
_cons	2.10	0.07	28.18	0	1.96	2.25
_IsenXtre_1_1 + _Itreatment_1	.40	.0261934	15.19	0.000	.35	.45

[a]Data are arranged for input into STATA14 statistical software. "0" represents cells treated with 0 nM FK866. "1" represents cells treated with 10 nM FK866. The fl values represent the geometric mean from 488/405 nm fluorescence ratio of the healthy, single HeLa cells measured by cytometry. Experiment, biological replicate; fl, 488/405 nm geometric mean fluorescent value; treatment, ±10 nM FK866; sensor, ±cytoplasmic NAD^+ sensor.
[b]The *p*-value for the ratio-of-ratios across replicates (bold) is reported under the statistical interaction "_IsenXtre_1_1". This represents the fluorescence change following FK866 treatment in the cytoplasmic sensor, relative to changes in cpVenus. Calculating the exponential of the coefficient value, Coef., represents the mean fold-change in fluorescence for the ratio of ratios, across replicates, i.e., e^(0.40) = 1.49, 95% CI (1.38 to 1.60), $p < 0.001$.The fluorescence change in cytoplasmic cpVenus with treatment across replicates is represented by the "_Itreatment_1" row: e^(coef) = e^(0.00) = 1.00, $p = 0.982$.To calculate the fluorescent change in cytoplasmic sensor independent of cpVenus, combine the "treatment" and "sensor X treatment interaction" using the lincom command (step 50). The combined values (blue) represents the change in the sensor: e^(coef) = e^(0.40) = 1.49, 95% CI (1.42 to 1.57), $p < 0.001$.

ALTERNATE PROTOCOL

CALIBRATION OF SENSOR FLUORESCENCE TO INTRACELLULAR NAD^+ CONCENTRATIONS

Apart from evaluating relative changes in steady-state NAD^+ levels between control and experimental conditions, the sensor can be used to ascribe quantitative measurements to these changes. To accomplish this, the fluorescence of the sensor needs to be calibrated with known NAD^+ concentrations to generate a standard curve. Experimental fluorescence readings (488/405 nm) are then interpolated from the reference curve to obtain NAD^+ measurements. For accuracy, a standard curve must be generated for each instrument setup and should be repeated if there are changes in instrumentation. As NAD^+ is intrinsically acidic, this approach requires a buffered NAD^+ stock solution, which is described in steps 1 through 4.

The approach for calibration described here involves acutely permeabilizing cells using digitonin such that internal stores of NAD^+ equilibrate with externally provided

Table 6 Data and Statistical Analysis from Mitochondrial Sensor Replicates

Data represents biological replicates using transiently transfected mitochondrial sensor and mitochondrial cpVenus in HeLa cells[a]

Experimen	fl	Treatment	Sensor
1	24.9	0	0
1	23.4	1	0
1	7.01	0	1
1	8.41	1	1
2	22.1	0	0
2	22.8	1	0
2	5.37	0	1
2	7.30	1	1
3	20.4	0	0
3	23.8	1	0
3	4.61	0	1
3	6.76	1	1

Calculated statistical interaction table from STATA14 using REML[b]

log_fl	*Coef.*	*Std. Err.*	*z*	*P*> |*z*|	*[95% Conf.*	*Interval]*
_Isensor_1	−1.39	0.07	−19	0	−1.53	−1.25
_Itreatment_1	0.04	0.07	0.56	0.574	−0.10	0.18
_IsenXtre_1_1	0.25	0.10	2.41	**0.016**	0.05	0.45
_cons	3.11	0.08	41.36	0	2.96	3.26
_IsenXtre_1_1 + _Itreatment_1	0.29	0.07	3.97	0	0.15	0.43

[a]Data are arranged for input into STATA14 statistical software. "0" represents cells treated with 0 nM FK866. "1" represents cells treated with 10 nM FK866. The fl values represent the geometric mean from 488/405 nm fluorescence ratio of the healthy, single HeLa cells measured by cytometry. Experiment, biological replicate; fl, 488/405 nm geometric mean fluorescent value; treatment, ±10 nM FK866; sensor, ±mitochondrial NAD^+ sensor.
[b]The *p*-value for the ratio-of-ratios across replicates (bold) is reported under the statistical interaction "_IsenXtre_1_1". This represents the fluorescence change with treatment in the mitochondrial sensor, relative to changes in cpVenus. Calculating the exponential of the coefficient value, Coef., represents the mean fold-change in fluorescence for the ratio-of-ratios across replicates, i.e., e^(0.25) = 1.28, 95% CI (1.05 to 1.57), $p = 0.016$.The fluorescence change upon treatment in nuclear cpVenus across replicates is represented by "_Itreatment_1": e^(coef) = e^(0.04) = 1.04, $p = 0.574$.To calculate the average fluorescent change in the mitochondrial sensor independent of cpVenus, combine the "treatment" and "sensor X treatment interaction" using the lincom command (step 50). The combined values (blue) represents the change in the sensor: e^(coef) = e^(0.29) = 1.34, 95% CI (1.16 to 1.54), $p < 0.001$.

concentrations of NAD^+ (Cambronne et al., 2016, Zhao et al., 2011). Equilibration of cells is monitored by internalization of the molecular dye, propidium iodide (PI), which has a similar molecular weight to NAD^+. When PI is excited at 561 nm, it emits a fluorescence that can be monitored with a 670 ± 15-nm filter. This excitation and filter combination permits PI fluorescence to be simultaneously monitored with the fluorescence of the sensor in the same cell. Measurements of the sensor's 488/405 nm fluorescence in PI-positive cells can then be correlated with applied NAD^+ concentrations to generate a calibration curve. Sensor measurements used to generate an in-cell calibration curve can be obtained from 10-cm plates of cells transiently transfected the previous day with cytoplasmically localized cpVenus or sensor. It may be technically easier and more cost-effective, nevertheless, to use stably expressing cell lines of the cytoplasmic cpVenus or sensor (Fig. 3).

Additional Materials *(also see Basic Protocol)*

β-Nicotinamide adenine dinucleotide hydrate (NAD^+, see recipe)
Dilution buffer (see recipe)
1 N sodium hydroxide (NaOH, Fisher Scientific, cat. no. SS2661)
HEK293T cells (healthy, proliferating, and maintained in 10-cm dish or similar)
Propidium iodide (668.39 g/ml, Sigma, cat. no. P4170), prepare 10 mg/ml in PBS, aliquot, and store in dark at −20°C; dilute immediately prior to use
5% (w/v) digitonin (Thermo Fisher, cat. no. BN2006), store at 4°C; heat 30 sec to 2 min at 95°C and vortex to re-dissolve prior to use

MColorpHast 5.0 to 10.0 pH–indicator strips (Millipore, cat. no. 109533)
5-ml polystyrene round-bottom tubes (Corning, cat. no. 352235)

Generate buffered 50 mM NAD^+ stock at pH 7.4

1. Resuspend 25 mg NAD^+ in 500 µl dilution buffer.

   The dilution buffer composition is important, as NAD^+ is unstable in phosphate buffers (Anderson & Anderson, 1963), and addition of salt mimics physiological concentrations.

2. Increase the pH with ∼25 µl of 1 N NaOH to approximately pH 6.5. Then, slowly add 0.1 N NaOH (∼10 µl) to increase pH ∼7.5. Mix well and use pH strips to confirm pH.

3. To the total volume of ∼535 µl, bring volume up to 753.66 µl total with dilution buffer for a 50 mM stock. Mix well.

4. Dispense into 25- to 50-µl aliquots and store up to 1 year at –20° or –80°C.

Determine experimental conditions and digitonin concentration

5. Determine the appropriate concentration of digitonin for permeabilization. Trypsinize and collect HEK293T cells from an 80% to 90% confluent 10-cm plate into 5 ml of cell culture growth medium. Count cells and adjust volume so that cells are resuspended at a concentration of 1×10^6 cells per milliliter cell culture growth medium.

   A more concentrated or less concentrated cell suspension can be used, but this will affect the required amount to digitonin. A concentration of 1×10^6 HEK293T cells per milliliter is recommended as an appropriate starting concentration that can be permeabilized by 0.001% v/v digitonin in 15 min at room temperature.

6. Set aside 500 µl of cell suspension for PI-negative cells (no-PI control).

   This control is required to ascertain the difference between ± PI internalization.

7. Remove 5 ml of cell suspension and add 10 µl of 15 mM PI stock, such that final concentration of PI is 30 µM. Vortex to mix well.

8. Prepare and label nine 5-ml polystyrene round-bottom tubes with the following indicated digitonin concentrations: 0%, 0.00010%, 0.00025%, 0.00050%, 0.00075%, 0.00100%, 0.00125%, 0.00150%, and 0.00175% v/v.

9. Pipet 500 µl of the cell/PI mixture into each of the pre-labeled polystyrene round-bottom tubes and set these aside.

10. Analyze the no-PI control cells on a flow cytometer to set gates for live cells of uniform side and forward scatter (P1) and single cells (P2, from P1). From the single-cell population (P2), select the *y*-axis to read the FSC-A (linear) and the *x*-axis to monitor PI fluorescence following excitation at 561 nm and using emission

filter 670 ± 15 nm (log). Using the no-PI control as a guide, draw a gate that excludes that population and only includes PI-positive cells (P4). (Fig. 4)

11. Analyze the 0% digitonin cell/PI mixture. If any PI-staining is observed in this sample, it indicates membrane-compromised and, likely, unhealthy cells. Unhealthy cells are characterized by strong PI-staining and should be excluded from the P4 gate. In contrast, when cells are permeabilized and equilibrated with PI (as will be observed in subsequent steps) the staining is less intense and is only present in digitonin-permeabilized samples. Use this sample to define the P4 gate to also exclude the unhealthy high-PI cells (Fig. 4).

12. Using a 0.05% v/v digitonin stock—which has been serially diluted from the 5% w/v digitonin stock in dilution buffer—calculate the appropriate volume of digitonin for each percentage to be tested. Add this volume to the appropriate 500-µl cell/PI aliquot. Vortex to mix and incubate 15 min at room temperature.

    It is critical to incubate each sample for exactly the same amount of time, so addition of digitonin is staggered such that analysis can be performed at the 15-min mark. The 15-min mark was empirically determined to be a sufficient amount of time such that PI could internally equilibrate while cells remained viable.

13. After 15 min, analyze each sample. Collect 10,000 cells in the P2 gate, record the percentage of P2 cells in the P4 gate (PI+).

14. Plot a semi-log graph with the percentage of digitonin on the *x*-axis and the percentage of PI-positive cells on the *y*-axis. Examples of this are available in Cambronne et al. (2016), Figure S11 and Zhao et al.(2011), Figure 2E. The lowest amount of digitonin required to equilibrate the population is the amount to use to generate the calibration curve. It has previously been found that 0.001% v/v is typically an appropriate amount to permeabilize HEK293T cells at a concentration of 1×10^6 cells per milliliter.

Monitor fluorescence of sensor in the PI-equilibrated population

15. Prior to monitoring the responses to NAD^+ by the sensor and cpVenus, define the P5 gate using untransfected or parental cells that do not express any fluorescent protein by utilizing the same samples that were used to determine an appropriate digitonin concentration in steps 5 through 14. The P5 gate defines the fluorescent population and is derived from the P4 (PI+) population. It is defined by exclusion of cells in the non-fluorescent sample, and inclusion of cells wherein cpVenus or sensor proteins are expressed (Fig. 4). To define P5, analyze the P4 population (PI+) on a new plot. Set the *x*-axis display to log format with excitation at 405 nm and the emission filter set 525 ± 25 nm. Set the *y*-axis display to log format with excitation at 488 nm and the emission filter set 530 ± 15 nm. Ratiometric fluorescent measurements of the sensor and cpVenus (488/405 nm) will be obtained from the P5 population.

Calibrate in-cell sensor fluorescence to NAD^+ concentrations

This calibration requires 10-cm dishes of cells each expressing either cytoplasmic localized cpVenus or sensor. It is possible to use 10-cm dishes of cells that have been previously transiently transfected for either cytoplasmic cpVenus or sensor, or use stably expressing lines (Fig. 3). To generate stably expressing lines, refer to the protocol provided in Lai, Yang, and Ng (2013). These expression plasmids are compatible for lenti-viral production using 2nd generation viral helpers. This calibration is best suited for cytoplasmic measurements.

16. Label polystyrene flow cytometry round-bottom tubes with the range of NAD^+ concentrations to be tested. Start with the following concentrations: 10 µM, 30 µM, 100 µM, 300 µM, 1 mM, 3 mM, and 10 mM.

17. Dilute NAD^+ stock in buffer to represent the 5× experimental values to test, e.g., to measure effects of 100 μM NAD^+, dilute the NAD^+ to a 5× stock of 500 μM NAD^+. Pipet 100 μl of 5× stocks into appropriate, pre-labeled tubes. Set aside these tubes (to be eventually mixed with 400-μl aliquot of a cell/PI/digitonin suspension).

18. Trypsinize with 1 ml of 0.05% trypsin for 5 min and collect cells from a 10-cm dish that is 80% to 90% confluent. Count cells and resuspend them at a concentration of $\sim 1 \times 10^6$ per milliliter cell culture growth medium. A minimum of 5.5 ml is required for nine data points; to account for pipetting error, prepare 6 ml. Collect and analyze one cell line at a time, either sensor or cpVenus, to facilitate and maintain consistent timing.

19. Remove 500 μl of cell suspension as a PI- or digitonin-negative control. Use this control to set and confirm P1 and P2 gates for uniform and single cell populations, respectively.

20. Add PI to the remaining 5.5 ml of cell suspension for a final concentration of 30 μM.

21. Remove 500 μl of cell/PI suspension as a control condition (PI, no digitonin). Analyze this sample to define P4 as previously outlined in steps 10 and 11 (Fig. 4).

22. To the remainder of the cells (5 ml), add 12.5 μl of 0.05% v/v digitonin stock, such that the final percentage is 0.00125% v/v, or 1.25× the required digitonin concentration that was empirically determined. When 400 μl of this cell/PI/digitonin suspension is mixed with 100 μl of the diluted NAD^+, the final concentration of digitonin will be 0.001% v/v. Once the digitonin has been added, immediately vortex and distribute 400 μl of the cells/PI/digitonin suspension to the each pre-labeled tube that already contains 100 μl of 5× NAD^+.

Staggered preparation of sample is critical for ensuring accurate timing for each sample.

23. Vortex the cell/PI/digitonin/NAD^+ mixture and incubate 15 min at room temperature.

24. Analyze samples and collect 10,000 events from P5.

25. Complete the flow cytometry analysis of all samples from each cell line within 5 to 10 min from each other for accurate measurements.

26. (Pause Point) On a semi-log graph, plot the log NAD^+ concentrations on the *x*-axis and the ratio-of-ratio sensor/cpVenus (488/405 nm) values on the *y*-axis. Examples of expected changes can be found in Cambronne et al. (2016), Figure S12.

27. Biological replicates can be fit to a sigmoidal regression model $y = min + [\frac{(min - max)}{1+10^{(logEC50-x)hillslope}}]$ and 95% confidence intervals calculated. Ratio-of-ratio *y* measurements can be interpolated onto this curve to obtain values for *x*.

REAGENTS AND SOLUTIONS

Cell culture growth medium

Dulbecco's modified Eagle medium (DMEM) containing 4.5 g/liter D-glucose and 110 mg/liter sodium pyruvate (Thermo Fisher, cat. no. 11995-065)
10% v/v fetal bovine serum (FBS, Thermo Fisher, cat. no. 10437028)
25 mM HEPES (1 M HEPES buffered solution, pH 7.4; Thermo Fisher, cat. no. 15630080)

Under sterile conditions in a tissue culture hood, add 50 ml FBS to 500 ml DMEM medium. Add 12.5 ml HEPES buffer, pH 7.4, to medium and mix. Store up to 1 month (if unopened) at 4°C.

Dilution buffer (100 mM Tris·Cl, pH 7.4/150 mM NaCl)

Dilute 5 ml of 1 M Tris·Cl, pH 7.4 and 1.5 ml of 5 M NaCl with 43.5 ml ultrapure water (total volume 50 ml). Filter sterilize using a 0.22-μm filter to remove dust and particulates. Store up to 2 years at room temperature (20° to 25°C).

FK866, 50 mM

To prepare a stock of 50 mM FK866 (Cayman Chemical, cat. no. 13287), add 255 μl DMSO (Fisher Chemicals, cat. no. 67-68-5) to 5 mg FK866 powder. Vortex to mix. Serially dilute fresh to final concentration of 10 nM. Store up to 1 year at –20°C in 50-μl aliquots.

Serially dilute in cell culture growth medium (see recipe) to 10 nM working concentration immediately before use. Do not store aqueous dilutions for >24 hr.

NAD^+ stock, 50 mM

Resuspend 25 mg of NAD^+ (>99% pure NAD^+, Sigma, cat. no. N1636) in 500 μl dilution buffer (see recipe). Add ~25 μl of 1 N NaOH at approximately pH 6.5, then slowly add 0.1 N NaOH (~10 μl) to increase pH ~7.5. Mix well and use pH strips to confirm pH. Add volume up to 753.66 μl total with dilution buffer (see recipe) for a 50 mM stock. Mix well, aliquot into 25- to 50-μl aliquots, and freeze for up to 1 year at −20°C or −80°C.

COMMENTARY

Background Information

In the late 1990s, the Tsein laboratory found that GFP-like proteins could maintain fluorescence despite permutation of the primary sequence and even tolerate large peptide insertions, as long as its beta-barrel structure was intact to protect the fluorophore (Baird, Zacharias, & Tsien, 1999). By inserting calmodulin into eYFP, Baird et al. (1999) pioneered the first single-FP (fluorescent protein) sensor for calcium. This was further developed into a ratiometric intracellular Ca^{2+} sensor by Miyawaki, Nagai, and colleagues (Nagai, Sawano, Park, & Miyawaki, 2001), which set the groundwork for the GECO and GCaMP sensor series commonly used today (Akerboom et al., 2012; Chen et al., 2013; Tian et al., 2009; Wu et al., 2014; Zhao et al., 2011), and also represents the strategy that has been subsequently utilized in many other single fluorescent–protein biosensor designs, including those used for the NADH:NAD^+ sensors (Bilan et al., 2014; Hung, Albeck, Tantama, & Yellen, 2011; Zhao et al., 2011; Zhao et al., 2015).

The NAD^+ sensor combines a circularly permuted fluorescent protein (cpVenus) with a binding domain for NAD^+ (Fig. 2A). This unique bi-partite NAD^+ binding domain was modeled after the NAD^+-binding of bacterial DNA ligase, which specifically binds NAD^+ and undergoes a conformational change upon NAD^+ binding (Gajiwala & Pinko, 2004; Lahiri et al., 2012). Attachment of an NAD^+-binding domain to cpVenus physically links the fluorescence of the cpVenus chromophore to local NAD^+ availability. In other words, binding of free NAD^+, representing its local availability, in turn affects fluorescence from the chromophore of the sensor resulting in decreased fluorescence. The binding pocket was further engineered to ensure reversible and non-destructive binding of NAD^+. Overall, the sensor was shown to be specific for NAD^+ relative to NADH, uniquely bound the free fraction, and could measure NAD^+ within its estimated physiological range. For this NAD^+sensor, increasing NAD^+ availability decreases the fluorescence intensity of the sensor (Fig. 2). Thus, there is an inverse relationship between the fluorescence intensity of the sensor and the free NAD^+ concentration that can be reliably detected between ~30 μM and 1 mM. Because the sensor is genetically encoded, subcellular localization sequences can be incorporated to target the sensor to specific subcellular compartments to determine local NAD^+ measurements (Cambronne et al., 2016).

Methods to measure free NAD^+ are needed because unlike NADH—whose free fraction can be distinguished from protein-bound NADH in cells due to distinct differences in intrinsic fluorescence lifetimes (Patterson, Knobel, Arkhammar, Thastrup, & Piston, 2000; Zhang, Piston, & Goodman, 2002)—the

oxidized NAD^+ molecule has no intrinsic fluorescence. Moreover, estimates of free NAD^+, using free NADH or NADH/NAD^+ measurements are unlikely to accurately reflect free NAD^+ concentrations because of a high NAD^+/NADH ratio in most subcellular compartments. In mammalian cells, the ratio of free NAD^+ to NADH is estimated at ~700:1 in the nucleocytoplasm, and ~7:1 in mitochondria (Williamson et al., 1967). Due to their disproportionate ratio and because the concentration of free NAD^+ exceeds that of free NADH, current ratiometric NADH:NAD^+ sensors are prone to saturation for NAD^+ when used in cells (Bilan et al., 2014; Hung et al., 2011; Zhao et al., 2011; Zhao et al., 2015. Monitoring changes in free NADH can overestimate the resulting changes in NAD^+ concentrations.

Approaches to directly detect the free NAD^+ relevant for cellular signaling pathways would additionally need to provide information about its subcellular measurements. NAD^+ is highly compartmentalized and its levels are maintained at distinct steady-state concentrations in different subcellular compartments (Cambronne et al., 2016; Pittelli et al., 2010; Yang et al., 2007). Regulation of these subcellular pools is complex due to the multiple and paralogous biosynthetic and consuming enzymes that are differentially expressed according to cell or tissue type (Cambronne et al., 2016; Felici, Lapucci, Ramazzotti, & Chiarugi, 2013; Mori et al., 2014), as well as differentially localized within subcellular compartments (Berger, Lau, Dahlmann, & Ziegler, 2005; Mori et al., 2014; Nikiforov, Dölle, Niere, & Ziegler, 2011; Raffaelli et al., 2002). Moreover, the rates of individual enzymes can be controlled independently (Berger et al., 2005; Nikiforov et al., 2011; Raffaelli et al., 2002; Sorci et al., 2007). Thus, local concentrations of NAD^+ can differ in different biological compartments and subcellular concentrations of NAD^+ can be regulated independently through biosynthetic pathways or depleted by the previously mentioned local consuming enzymes (Fig. 1). Methods that rely on preparation of cellular extracts—such as liquid-chromatography mass spectrometry, or colorimetric or fluorogenic assays—often compromise spatial information and it is usually unclear what proportion of the collected pool represents the free NAD^+ fraction. Magnetic resonance scanning can distinguish NAD^+ from NADH and has been used for patient diagnosis (Zhu, Lu, Lee, Ugurbil, & Chen, 2015), but it cannot distinguish bound from free fractions and is limited for subcellular interrogations. Lastly, while both indirect readouts such as the PARAPLAY assay (Dölle, Niere, Lohndal, & Ziegler, 2010) or direct NAD^+ measurements using a semisynthetic sensor (Sallin et al., 2018) have been extremely informative, the authors' emphasis has been to develop a completely genetically encoded method to directly detect free intracellular NAD^+.

Critical Parameters

There are two important controls required when using the NAD^+ sensor. Distinct from the brighter fluorescence that follows excitation at 488 nm and represents NAD^+-dependent changes, it is also recommended to take a secondary measurement of fluorescence between ~500 and 525 nm following excitation at 405 nm (Fig. 2B). Fluorescence after excitation at 405 nm proportionally tracks *in vitro* with the abundance of the sensor or cpVenus, and thus its intensity can be used for normalization of sensor expression levels in cells (Cambronne et al., 2016). The second important control is cpVenus alone (without the NAD^+ binding pocket), whose fluorescence is not affected by NAD^+ (Cambronne et al., 2016). It was found that pH influences the fluorescence of the sensor and cpVenus control similarly between pH conditions 6.6 and 8.0 (Cambronne et al., 2016). Thus, parallel analysis of fluorescent changes in cpVenus can be used to normalize for pH effects and other non-specific changes in fluorescence within this range (Bilan et al., 2014, Cambronne et al., 2016). Most intracellular compartments fall within this pH range, including the nucleus, cytosol, mitochondria, peroxisomes, endoplasmic reticulum, and the *cis*-golgi network (Casey et al., 2010). Complete cell culture growth medium used to resuspend cells prior to analysis must be made fresh such that it is within near-neutral pH. Media that is not near neutral pH is unable to sufficiently buffer the cell suspension for the duration of the flow analysis. If media contains phenol red, it should be orange-red in color without any traces of pink or magenta and is ideally opened and supplemented immediately before analysis. Phenol red will not interfere with flow analysis because cells are diluted in sheath buffer during the analysis. To confirm experimental and instrumental setups for sensor measurements, utilize FK866 to deplete intracellular NAD^+.

Similar to other FP sensors, this NAD^+ sensor is sensitive to the pH of its environment, and thus incompatible with cell compartments

pH <6.5, including the *trans*-golgi network, secretory granules, endosomes, and lysosomes (Casey, Grinstein, & Orlowski, 2010). In cases when the pH of a compartment is low, overall fluorescence is eliminated both from cpVenus and the sensor (Cambronne et al., 2016). Thus, a general limitation of the sensor is that it cannot monitor NAD^+ under experimental conditions that would eliminate overall fluorescence, e.g., pH <6.5 or exogenous H_2O_2. NAD^+-dependent changes only alter and do not completely eliminate fluorescence, so a lack of fluorescence from both cpVenus and the sensor would indicate experimental conditions where the sensor cannot measure NAD^+. This point highlights the necessity of the cpVenus parallel control.

Currently, the response time of the sensor to respond to NAD^+ fluctuations is unknown. This has not been a limitation in the measurements, but the time lag has not been formally defined. The sensor also has a limited sensitivity when measuring NAD^+ levels outside the range of 30 μM to 1 mM. The dynamic range of fluorescence for the sensor is ∼50%, corresponding to a ∼30% increase or ∼20% decrease in fluorescence (Cambronne et al., 2016). Measurements of modest changes can be improved by reproducibility in measurements of a large sample size, facilitated by flow cytometry approaches.

The NAD^+ sensor is compatible with common instrumentation setups and has unique and advantageous properties over previously determined methods.

At extreme supra-physiological concentrations, NAD^+ precursor molecules NR and NMN can influence the sensor. To the authors' knowledge, the extent to which steady-state intracellular NMN or NR increases intracellularly upon exogenous treatments is currently still unknown. Notwithstanding, it was found that 25 μM NMN (25× supra-physiological) and 100 μM NR (>6000× supra-physiological) only minimally affected the NAD^+ sensor *in vitro*, and so it is recommended to use these concentrations to exogenously treat cells when sensor measurements are taken. It is also critical to prepare media for the experiment as listed in the Reagents and Solutions section.

This version of the sensor may have limited sensitivity to reliably detect modest NAD^+ changes, and the apparent sensitivity of the sensor also depends on how well the particular instrumentation can detect fluorescence. As standard practice when using flow cytometry, it is recommended to analyze 10,000 fluorescent cells per condition. An analysis using a power of 90% and data obtained on the cytometer indicated that this was sufficient to distinguish changes in all examined compartments. A list of recommended filter sets to use for experimental measurements is provided. A straightforward approach using the small molecule FK866, an NAMPT inhibitor, to check instrument capabilities is provided. It is highly recommended to use this positive test before moving onto experimental conditions.

Troubleshooting

FK866 treatment

If treated cells are unhealthy (Fig. 4) or have aberrant morphology (1) FK866 concentration may be too high. Re-confirm calculation of serial dilutions. Dilute fresh in medium or can test different concentrations. (2) FK866 incubation exceeded 18 hr. Ensure that evaluation is performed within 18 hr.

If treatment has no effect (1) it may be due to incorrect FK866 concentration or incubation time. Re-confirm calculation of serial dilutions. Dilute in fresh medium right before use. (2) It may be due to incorrect FK866 concentration because too much growth medium was left in well. Remove growth medium completely and replace with 10 nM FK866 final concentration. (3) FK866 was not properly stored. Remake stock in DMSO, aliquot, and store at –20°C. Can confirm efficacy of FK866 treatment by whole cell chromatography, which should be able to detect depletion of total cellular NAD^+. (4) Insufficient buffering of the samples during analysis. Use freshly made medium containing HEPES to collect cells and confirm that medium is orange-red in color. Minimize the time it takes to analyze samples by performing small batches and having the instrument ready ahead of time.

In-cell calibration

If fluorescence of cpVenus is altered upon equilibration with high concentrations of NAD^+, then NAD^+ stock solution may not be sufficiently buffered and remains slightly acidic. Remake NAD^+ stock solution and ensure that the final stock solution containing Tris·Cl and NaCl is buffered accurately to pH 7.4. When further diluted to make the 5× stock, acidity should remain at pH 7.4.

If the sensor or cpVenus cells lose fluorescence upon permeabilization but without the addition of NAD^+: (1) cells are unhealthy or dying. Try equilibrating with less digitonin.

Re-establish the minimal amount of digitonin required to permeabilize the cell type. It may also be necessary to shorten the incubation time before analysis (see below). (2) Inadvertent introduction of quencher. Ensure that none of the buffers, instrument buffers, or reagents contains any compounds that can quench fluorescence.

If cells are dying before measurements can be obtained, then (1) there may be too much digitonin. Re-establish and use the minimal concentration of digitonin required to allow for PI-equilibration within 15 min for each cell type. (2) Impure digitonin stock. Use only highly pure digitonin from source that has been recrystallized or from a stock that is >99% pure. Digitonin should readily go into aqueous solution at 5% and should be clear. Digitonin can be recrystallized to improve its purity. Digitonin is first dissolved in ethanol at 75°C, precipitated in ice water for 20 min, and centrifuged to form a pellet. Repetition of these steps two times can result in ∼60% recovery that is isolated by vacuum drying. Weighed material is now pure enough for use. (3) Too long of an incubation. Once cells are equilibrated, consistently maintain the incubation time for all samples to ∼15 min. This can be achieved by staggering the addition of digitonin and analysis among the samples. (4) Precipitated digitonin resulting in inconsistent permeabilization. Warm up digitonin solution in a 90° to 95°C water bath/heat block and vortex to re-solubilize the digitonin into a clear solution. This should ensure accurate application of digitonin.

If there is no observation of PI-equilibrated cells, then (1) it may be due to insufficient digitonin concentration for cell type. Establish minimum effective digitonin concentration to equilibrate intracellular PI within 15 min for specific cell type (see Alternate Protocol, step 22). (2) Incorrect laser excitation or fluorescent filter set. Confirm that an appropriate excitation laser and filter set is being used. (3) Accidental omission of PI dye. Confirm that PI has been added to sample. (4) May have missed the proper timepoint. Establish timepoints with the incubation time required for the specific cell type.

If measurements are off-scale of calibration curve, then (1) lower scale measurements that require substantial NAD^+ diffusion out of the cell, they are a limitation for this in-cell calibration method. A bead-based calibration of the instrumentation can be used for this low range (Cohen et al., 2018). (2) Instrument has been changed. Determine whether there have been any adjustments or calibration of laser settings, voltages, or alignments in between experimental replicates. Calibration can be repeated for new instrumental settings. Replicates should be all obtained under the same configuration that will also be used for data collection.

If there is an insufficient number of fluorescent cells, then transfection efficiency was too low. Use a stably expressing line to ensure that all cells that are PI-equilibrated in P4 will be fluorescent in P5.

If a large standard deviation in replicates when generating calibration curve occur, then experimental inconsistencies that may include incubation timing, NAD^+ concentrations, and permeabilization of cells. Ensure that the 15-min incubation time with NAD^+ and digitonin is always consistent among samples. This can be achieved by staggering the addition of digitonin and NAD^+. Confirm that NAD^+ stock concentrations are consistent across experiments and that the NAD^+ has not degraded. Using freshly diluted 5× stocks aids in consistent pipetting. Confirm that the digitonin stock is pure and has not precipitated.

Statistical analysis

If the FK866 results are not statistically significant, then there is too much variability among replicates. Use freshly made medium to collect cells each time. Minimize the time it takes to analyze samples by performing small batches and having the instrument ready ahead of time. Because the absolute values of the measurements depend on the specific instrument and lasers, ensure that replicates are performed on the same instrument with exactly the same settings.

If fluorescence from cpVenus is changing then the pH across samples is not sufficiently stabilized. Phenol-red indicator in medium will turn from orange to pink. Confirm that collection medium contains HEPES. Use freshly made orange-red medium (but not yellow-red) to collect cells each time. Minimize the time it takes to analyze samples by performing small batches, running on high, having high transfection efficiency, and having the instrument ready ahead of time. Also ensure that all samples are analyzed at the same temperature. It may be preferable to keep samples chilled until immediately before analysis. Can overlay a thin layer of mineral oil atop each sample to minimize sample exposure to air.

If command is not recognized, then data was not uploaded correctly or with different headings. Confirm that correct data was

uploaded in data editor and headings are identical to what is used in command line.

Flow cytometry

If you cannot see cells. (1) Incorrect instrument setup. Make sure instrument setup is correct and lasers are on. Adjust voltages as needed. Can first view on log scale to find cells before changing to linear scale. (2) Clogged instrument. Potentially, unclog instrument by triturating cells and passing through a 0.45-μm nylon mesh to remove clumps. (3) No/few cells are detected as fluorescent. Poor transfection (see Transfection).

Flow analysis

If you cannot see events or gates. Events are off-scale. Adjust axis similarly to Fig. 4, both filter component and scale.

If gates or derived parameters are not applied to all samples. Did not apply to All Samples. Drag desired gate hierarchy or evaluation to All Samples heading on top.

If events do not look like example. Gates may not be organized as hierarchy. Make sure that gate P3 is defined from P2, and P2 is defined from P1.

If you cannot click on Derive Parameter option. When defining a new parameter, a specific subpopulation cannot be actively selected. Move cursor to deselect specific subpopulation.

Trypsinization

If cells will not detach from plate. Medium may not have been completely washed from dish. Try gently rinsing cells one additional time with PBS, aspirate completely before adding new trypsin.

Transfection

If there is poor transfection. Few fluorescent cells. (1) Low-quality DNA. Confirm with spectrophotometry a distinct and clear 260-nm peak, that the 260/280 nm ratio is ~1.8, and that the 260/230 nm ratio is ~2. Confirm by resolving the DNA on an agarose gel that the majority of the prep is supercoiled. Re-purify DNA using a maxiprep column and repeat transfection. (2) Incorrect DNA plasmid. Restriction digest analysis and sequencing can determine whether the plasmids are correct. Re-purify DNA as needed and repeat transfection. (3) Insufficient number of healthy cells. Ensure cells are at least 50% confluent and healthy before transfection and repeat transfection. Thaw new cells if necessary. (4) Did not incubate DNA and lipofectamine mixture for 20 to 30 min before adding to cells. Too little or too much incubation time of the DNA and Lipofectamine 2000 can affect transfection efficiency. Repeat transfection and keep track of incubation time. (5) Changed medium too soon after transfection. Incubate HeLa cells with transfection mixture for 2 hr.

If cells did not survive transfection: (1) low-quality DNA. Confirm with spectrophotometry a distinct and clear 260-nm peak, that the 260/280 nm ratio is ~1.8, and that the 260/230 nm ratio is ~2. Confirm by resolving the DNA on an agarose gel that the majority of the prep is supercoiled. Re-purify DNA using a maxiprep column and repeat transfection. (2) Forgot to change the medium 2 hr after transfection. Prepare new cells and transfection mixture and incubate HeLa cells with transfection mixture for 2 hr. (3) Forgot to use complete medium. Check that complete medium including serum was used. Start new transfection.

If you observe incorrect subcellular localization. (1) Incorrect DNA plasmid. Restriction digest analysis and sequencing can determine whether the plasmids are correct. Re-purify DNA as needed and repeat transfection. (2) Ectopic expression is too high, overwhelming endogenous targeting mechanisms. Re-transfect with half the amount of DNA and half the volume of Lipofectamine 2000.

Statistical Analyses

To evaluate the likelihood that any observed fluorescence changes occurred by chance, the data is analyzed by using a mixed-effects model (McCulloch, Searle, & Neuhaus, 2008) in which the experimental replicate is regarded as a random factor and the selective conditions of treatment and either sensor or cpVenus expression are both considered as fixed factors. Compared to other statistical evaluations, e.g., *t*-tests, this approach is most appropriate for estimating variance components of ratiometric measurements (Wulff, 2008). To help stabilize variance and limit the impact of outliers, first one log transforms the geometric mean fluorescence intensity value for the ratiometric 488/405 nm measurement. The requirement for this transformation is based on the observations that the untransformed data violates the model's assumptions of normality of the error distribution and homogeneity of error variances; log-transformed data showed no such violations. It is recommended to estimate variance by performing a Residual Maximum Likelihood (REML) analysis (Swallow, Monahan, 1984; Wulff, 2008). It is performed using the 488 nm/405 nm geometric mean

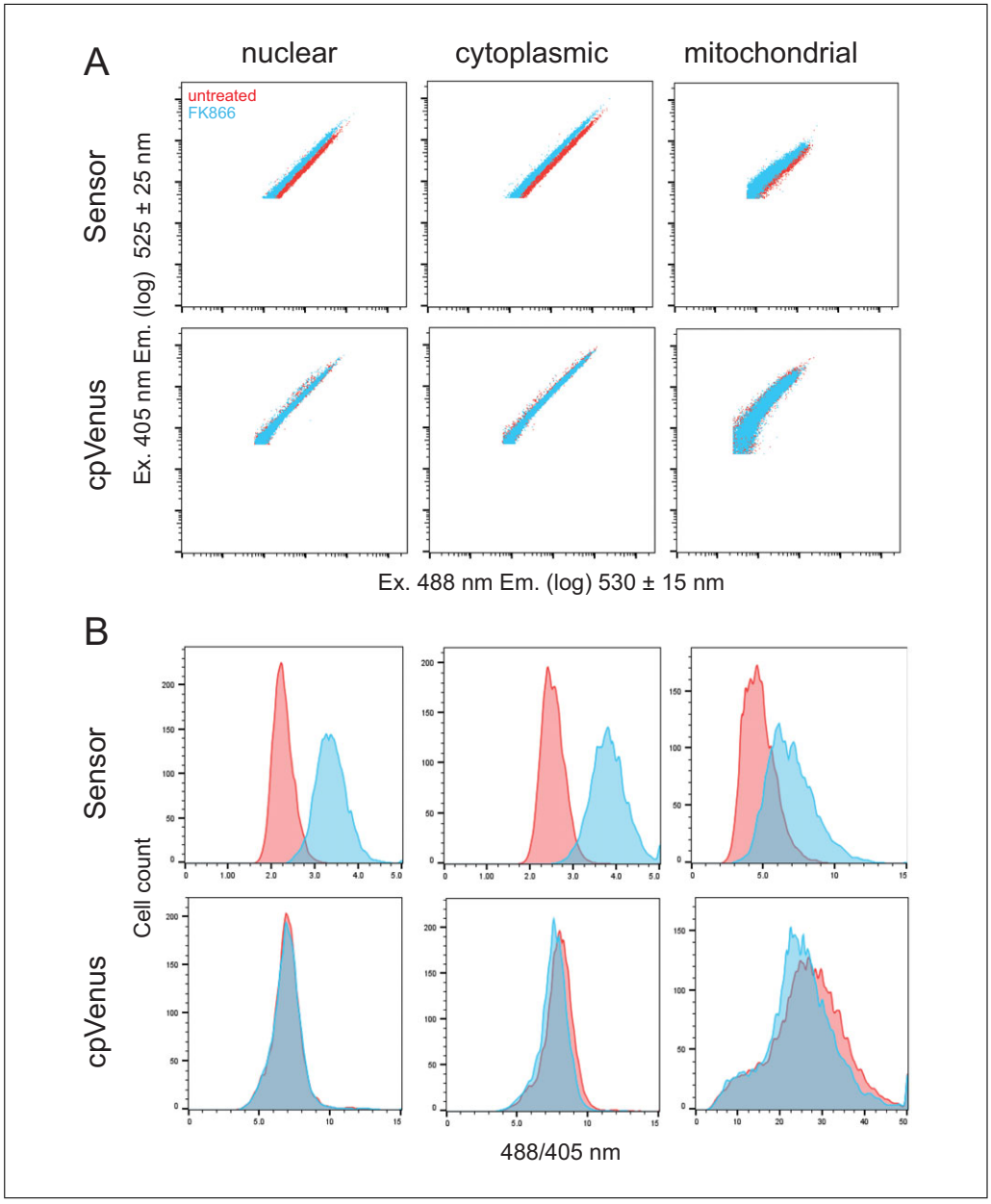

Figure 5 Representative data from cytometry measurements. (**A**) Logarithmic dot-plot fluorescent measurements of ~10,000 cells in P3 that have been transfected with plasmids expressing either the sensor or cpVenus, as indicated. Each column represents data determined from the indicated subcellular compartment. *x*-axis, fluorescence following 405-nm excitation; *y*-axis, fluorescence following 488-nm excitation. (**B**) Histograms showing the distribution of the same P3 population as a function of the 488/405 nm ratio per cell. Data was collected on a BD LSRII flow cytometer and analyzed on FlowJo V10 software.

values for each experimental condition, and a minimum of three biological replicates is required for sufficient power in the statistical analysis. A paired two-way ANOVA may also be appropriate, and this classical analysis is incorporated into many commonly-used statistical programs. However, advantages of REML include that its estimates of variance components are approximately unbiased even in small-sample settings, and that it separately fits the fixed and random effects and thus does not require a balanced experimental design for consistency of estimation (Wulff, 2008). An example of how to perform the REML statistical analysis using the commonly used STATA14 software is described (see Basic Protocol, steps 40 through 49).

Understanding Results

Cells treated with FK866 are unable to sufficiently replenish the NAD^+ that is turned over by NAD^+-consuming enzymes, and free

intracellular pools are depleted over time (Cambronne et al., 2016; Pittelli et al., 2010). It was found that 16 hr of FK866 treatment resulted in robust depletion of free NAD^+ in the subcellular compartments examined (Cambronne et al., 2016). Decreased NAD^+ concentrations result in brighter fluorescence intensity of the sensor after excitation at 488 nm, and minimally affect fluorescence after excitation at 405 nm (Cambronne et al., 2016). Thus, the brighter 488/405 nm fluorescence when measured per cell (derived parameter) in FK866-treated samples, compared to untreated samples, represents differences in NAD^+-availability that has been normalized for the expression of the sensor (Fig. 5 and Tables 4 through 6). Accordingly, the broad range in fluorescent intensities spanning the log scale that is due to transient transfection and varying plasmid copy number, collapses after normalization into a relatively tight peak on a linear scale representing the 488/405 nm fluorescence of that experimental sample (Fig. 5). NAD^+ concentrations do not affect fluorescence of the cpVenus protein (Cambronne et al., 2016), thus it is further normalized observed fluorescent changes to that of cpVenus subjected to the same experimental conditions (Fig. 5 and 4 through 6). This allows researchers to discern NAD^+-specific changes to fluorescence from non-specific factors influencing fluorescence. A detailed explanation of how to calculate and statistically evaluate the ratio of ratios is found in Basic Protocol, steps 31 through 49. Measurements can further be compared to a standard curve after the sensor is calibrated for a specific experimental setup. Calibration of the sensor is performed in parallel and described in the Alternate Protocol. By targeting the sensor to a specific subcellular compartment, the protocol described here for determining the fluorescent ratio of ratios provides a reliable method for monitoring changes in free NAD^+ concentrations in specific subcellular compartments.

Time Considerations

Basic Protocol

Seeding the cells (see Basic Protocol, steps 1 through 6) requires 30 min (day 1), transfection (steps 7 through 13) takes 2 to 3 hr (day 2), confirmation of expression and subcellular localization in stable cell lines or following transfection (step 14) takes 10 min (day 3), starting the 16-hr FK866 treatment (steps 15 to 17), requires 15 min (day 3), and defining gates and collecting flow cytometry measurements (steps 18 through 30) takes 20 to 30 min (day 4). The evaluation of ratio-of-ratios, statistical analysis (steps 31 through 49) is variable.

Alternate Protocol

In the Alternate Protocol, buffering NAD^+ stock (steps 1 through 4) requires 30 to 45 min. Determining experimental conditions and digitonin concentration (steps 5 through 15) takes 30 min to 2 hr (variable). Calibration of cpVenus and sensor-expressing cells with respect to equilibrated NAD^+ concentrations (steps 16 through 25) require ~1 hr per replicate analyzing both sensor- and cpVenus-expressing cells. The evaluation of ratio-of-ratios and generation of calibration curve (steps 26 and 27) varies in time.

Acknowledgements

The authors thank Mike Lasarev for his initial help guiding the statistical analysis and DongHo Kim for technical assistance in developing the sensor. Work was supported by the Hillcrest Committee, Pew Charitable Trust and the NIH (NS088629, UL1TR000128, P30CA069533, DP2GM126897). We apologize to all researchers whose primary works have not been cited owing to space constraints.

Conflicts of Interest

NAD^+ sensors are available from Oregon Health & Science University (OHSU) under a material transfer agreement with the authors. MLS, MSC, RHG, and XAC are inventors on patent application PCT/US15/62003 for the NAD^+ sensor.

Literature Cited

Akerboom, J., Chen, T. W., Wardill, T. J., Tian, L., Marvin, J. S., Mutlu, S., ... Looger, L. L. (2012). Optimization of a GCaMP calcium indicator for neural activity imaging. *The Journal of Neuroscience: The Official Journal of the Society for Neuroscience*, *32*(40), 13819–13840. doi: 10.1523/JNEUROSCI.2601-12.2012.

Anderson, B., & Anderson, C. (1963). The effect of buffers on nicotinamide adenine dinucleotide hydrolysis. *The Journal of Biological Chemistry*, *238*, 1475–1478.

Baird, G. S., Zacharias, D. A., & Tsien, R. Y. (1999). Circular permutation and receptor insertion within green fluorescent proteins. *PNAS*, *96*, 11241–11246. doi: 10.1073/pnas.96.20.11241.

Berger, F., Lau, C., Dahlmann, M., & Ziegler, M. (2005). Subcellular compartmentation and differential catalytic properties of the three human nicotinamide mononucleotide adenylyltransferase isoforms. *The Journal of Biological Chemistry*, *280*, 36334–36341. doi: 10.1074/jbc.M508660200.

Bilan, D. S., Matlashov, M. E., Gorokhovatsky, A. Y., Schultz, C., Enikolopov, G., & Belousov, V. V. (2014). Genetically encoded fluorescent indicator for imaging NAD(+)/NADH ratio changes in different cellular compartments. *Biochimica et Biophysica Acta*, *1840*(3), 951–957. doi: 10.1016/j.bbagen.2013.11.018.

Bucher, T., & Klingenberg, M. (1958). Wege des Wasserstoffs in der lebendigen Organisation. *Angew. Chem*, *70*, 552–570. doi: 10.1002/ange.19580701707.

Cambronne, X. A., Stewart, M., Kim, D., Jones-Brunette, A. M., Morgan, R. K., Farrens, D. L., ... Goodman, R. H. (2016). Biosensor reveals multiple sources for mitochondrial NAD^+. *Science*, *352*, 1474–1477. doi: 10.1126/science.aad5168.

Casey, J. R., Grinstein, S., & Orlowski, J. (2010). Sensors and regulators of intracellular pH. *Nature Reviews. Molecular Cell Biology*, *11*, 50–61. doi: 10.1038/nrm2820.

Chen, T.-W., Wardill, T. J., Sun, Y., Pulver, S. R., Renninger, S. L., Baohan, A., ... Kim, D. S. (2013). Ultrasensitive fluorescent proteins for imaging neuronal activity. *Nature*, *499*, 295. doi: 10.1038/nature12354.

Cohen, M. S., Stewart, M. L., Goodman, R. H., & Cambronne, X. A. (2018). Methods for Using a Genetically Encoded Fluorescent Biosensor to Monitor Nuclear NAD^+. In P. Chang (Ed.), *ADP-ribosylation and NAD^+ Utilizing Enzymes: Methods and Protocols* (pp. 391–414). New York, NY: Springer New York. https://doi.org/10.1007/978-1-4939-8588-3_26.

Dölle, C., Niere, M., Lohndal, E., & Ziegler, M. (2010). Visualization of subcellular NAD pools and intra-organellar protein localization by poly-ADP-ribose formation. *Cellular and Molecular Life Sciences : CMLS*, *67*, 433–443. doi: 10.1007/s00018-009-0190-4.

Felici, R., Lapucci, A., Ramazzotti, M., & Chiarugi, A. (2013). Insight into molecular and functional properties of NMNAT3 reveals new hints of NAD homeostasis within human mitochondria. *PLoS One*, *8*, e76938. doi: 10.1371/journal.pone.0076938.

Gajiwala, K. S. & Pinko, C. (2004). Structural rearrangement accompanying NAD^+ synthesis within a bacterial DNA ligase crystal. *Structure*, *12*, 1449–1459. doi: 10.1016/j.str.2004.05.017.

Gerdts, J., Brace, E. J., Sasaki, Y., DiAntonio, A., & Milbrandt, J. (2015). SARM1 activation triggers axon degeneration locally via NAD^+ destruction. *Science (New York, N.Y.)*, *348*(6233), 453–457. doi: 10.1126/science.1258366.

Holzer, H., Lynen, F., & Schultz, G. (1956). Determination of diphosphopyridine nucleotide/reduced diphosphopyridine nucleotide quotient in living yeast cells by analysis of constant alcohol and acetaldehyde concentrations. *Biochemische Zeitschrift*, *328*, 252–263.

Houtkooper, R. H., Cantó, C, Wanders, R. J., & Auwerx, J. (2010). The secret life of NAD^+: An old metabolite controlling new metabolic signaling pathways. *Endocrine Reviews*, *31*, 194–223. doi: 10.1210/er.2009-0026.

Hung, Y. P., Albeck, J. G., Tantama, M., & Yellen, G. (2011). Imaging cytosolic NADH-NAD(+) redox state with a genetically encoded fluorescent biosensor. *Cell Metabolism*, *14*(4), 545–554. doi: 10.1016/j.cmet.2011.08.012.

Lai, T., Yang, Y., & Ng, S. K. (2013). Advances in mammalian cell line development technologies for recombinant protein production. *Pharamceuticals*, *6*(5), 579–603. doi: 10.3390/ph6050579.

Lahiri, S. D., Gu, R.-F., Gao, N., Karantzeni, I., Walkup, G. K., & Mills, S. D. (2012). Structure guided understanding of NAD^+ recognition in bacterial DNA ligases. *ACS Chemical Biology*, *7*(3), 571–580. https://doi.org/10.1021/cb200392g.

McCulloch, C., Searle, S., & Neuhaus, J. (2008). *Generalized, Linear, and Mixed Models (2e)*. John Wiley & Sons. Hoboken, New Jersey.

Mori, V., Amici, A., Mazzola, F., Di Stefano, M., Conforti, L., Magni, G., ... Orsomando, G. (2014). Metabolic profiling of alternative NAD biosynthetic routes in mouse tissues. *PloS One*, *9*(11), e113939. doi: 10.1371/journal.pone.0113939.

Nagai, T., Sawano, A., Park, E. S., & Miyawaki, A. (2001). Circularly permuted green fluorescent proteins engineered to sense Ca2+. *PNAS*, *98*, 3197–3202. doi: 10.1073/pnas.051636098.

Nikiforov, A., Dölle, C., Niere, M., & Ziegler, M. (2011). Pathways and subcellular compartmentation of NAD biosynthesis in human cells: From entry of extracellular precursors to mitochondrial NAD generation. *The Journal of Biological Chemistry*, *286*, 21767–21778. doi: 10.1074/jbc.M110.213298.

Patterson, G. H., Knobel, S. M., Arkhammar, P., Thastrup, O., & Piston, D. W. (2000). Separation of the glucose-stimulated cytoplasmic and mitochondrial NAD(P)H responses in pancreatic islet beta cells. *Proceedings of the National Academy of Sciences of the United States of America*, *97*, 5203. doi: 10.1073/pnas.090098797.

Pittelli, M., Formentini, L., Faraco, G., Lapucci, A., Rapizzi, E., Cialdai, F., ... Chiarugi, A. (2010). Inhibition of nicotinamide phosphoribosyltransferase: Cellular bioenergetics reveals a mitochondrial insensitive NAD pool. *The Journal of Biological Chemistry*, *285*(44), 34106–34114. doi: 10.1074/jbc.M110.136739.

Raffaelli, N., Sorci, L., Amici, A., Emanuelli, M., Mazzola, F., & Magni, G. (2002). Identification of a novel human nicotinamide mononucleotide adenylyltransferase. *Biochemical and Biophysical Research Communications*, *297*(4), 835–840. doi: 10.1016/S0006-291X(02)02285-4.

Revollo, J. R., Grimm, A. A., & Imai, S. (2004). The NAD biosynthesis pathway mediated by nicotinamide phosphoribosyltransferase regulates Sir2 activity in mammalian cells. *The Journal of Biological Chemistry*, *279*, 50754–50763. doi: 10.1074/jbc.M408388200.

Sallin, O., Reymond, L., Gondrand, C., Raith, F., Koch, B., & Johnsson, K. (2018). Semisynthetic biosensors for mapping cellular concentrations of nicotinamide adenine dinucleotides. *eLife*, *7*, e32638. doi: 10.7554/eLife.32638.

Sorci, L., Cimadamore, F., Scotti, S., Petrelli, R., Cappellacci, L., Franchetti, P., ... Magni, G. (2007). Initial-rate kinetics of human NMN-adenylyltransferases: Substrate and metal ion specificity, inhibition by products and multi-substrate analogues, and isozyme contributions to NAD^+ biosynthesis. *Biochemistry*, *46*(16), 4912–4922. https://doi.org/10.1021/bi6023379 doi: 10.1021/bi6023379.

Swallow, W., & Monahan, J. (1984). Monte Carlo comparison of ANOVA, MIVQUE, REML, and ML estimators of variance components. *Technometrics*, *28*, 47–57 doi: 10.1080/0040 1706.1984.10487921.

Tian, L., Hires, S. A., Mao, T., Huber, D., Chiappe, M. E., Chalasani, S. H., ... Looger, L. L. (2009). Imaging neural activity in worms, flies and mice with improved GCaMP calcium indicators. *Nature Methods*, *6*(12), 875–881. doi: 10.1038/nmeth.1398.

Verdin, E. (2015). NAD^+ in aging, metabolism, and neurodegeneration. *Science*, *350*, 1208–1213. doi: 10.1126/science.aac4854.

Williamson, D. H., Lund, P., & Krebs, H. A. (1967). The redox state of free nicotinamide-adenine dinucleotide in the cytoplasm and mitochondria of rat liver. *The Biochemical Journal*, *103*, 514–527. doi: 10.1042/bj1030514.

Wu, J., Prole, D. L., Shen, Y., Lin, Z., Gnanasekaran, A., Liu, Y., ... (2014). Red fluorescent genetically encoded Ca2+ indicators for use in mitochondria and endoplasmic reticulum. *The Biochemical Journal*, *464*(1), 13–22. doi: 10.1042/BJ20140931.

Wulff, S. S. (2008). The equality of REML and ANOVA estimators of variance components in unbalanced normal classification models. *Statistics & Probability Letters*, *78*, 405–411. doi: 10.1016/j.spl.2007.07.013.

Yang, Y., & Sauve, A. A. (2016). NAD^+ metabolism: Bioenergetics, signaling and manipulation for therapy. *Biochimica et Biophysica Acta*, *1864*, 1787–1800. doi: 10.1016/j.bbapap. 2016.06.014.

Yang, H., Yang, T., Baur, J. A., Perez, E., Matsui, T., Carmona, J. J., ... Sinclair, D. A. (2007). Nutrient-sensitive mitochondrial NAD^+ levels dictate cell survival. *Cell*, *130*(6), 1095–1107. doi: 10.1016/j.cell.2007.07.035.

Zhang, Q., Piston, D. W., & Goodman, R. H. (2002). Regulation of corepressor function by nuclear NADH. *Science*, *295*, 1895–1897.

Zhao, Y., Hu, Q., Cheng, F., Su, N., Wang, A., Zou, Y., ... Yang, Y. (2015). SoNar, a highly responsive NAD^+/NADH sensor, allows high-throughput metabolic screening of anti-tumor agents. *Cell Metabolism*, *21*(5), 777–789. doi: 10.1016/j.cmet.2015.04.009.

Zhao, Y., Araki, S., Wu, J., Teramoto, T., Chang, Y. F., Nakano, M., ... Campbell, R. E. (2011). An expanded palette of genetically encoded Ca^{2+} indicators. *Science*, *333*(6051), 1888–1891. doi: 10.1126/science.1208592.

Zhao, Y., Jin, J., Hu, Q., Zhou, H. M., Yi, J., Yu, Z., ... Loscalzo, J. (2011). Genetically encoded fluorescent sensors for intracellular NADH detection. *Cell Metabolism*, *14*, 555–566. doi: 10.1016/j.cmet.2011.09.004.

Zhu, X. H., Lu, M., Lee, B. Y., Ugurbil, K., & Chen, W. (2015). In vivo NAD assay reveals the intracellular NAD contents and redox state in healthy human brain and their age dependences. *Proceedings of the National Academy of Sciences of the United States of America*, *112*, 2876–2881. doi: 10.1073/pnas.1417921112.

Key References

Cambronne, X. A., Stewart, M., Kim, D., Jones-Brunette, A. M., Morgan, R. K., Farrens, D. L., ... Goodman, R. H. (2016). Biosensor reveals multiple sources for mitochondrial NAD^+. *Science*, *352*, 1474–1477. doi: 10.1126/science. aad5168.

The NAD^+ sensor described in this protocol was originally published in Cambronne, et al. (2016).